

- ¹J. Agraz and S. S. Li, Phys. Rev. B 2, 4966 (1970).
²J. Agraz and S. S. Li, Phys. Rev. B 2, 1847 (1970).
³J. M. Fairfield and B. V. Gokehale, J. Solid State Electron. 8, 685 (1965).
⁴G. Bemski, Proc. IRE 46, 990 (1958).
⁵C. T. Sah, A. F. Tasch, Jr., and D. K. Schroder, Phys. Rev. Letters 19, 2 (1967); 19, 71 (1967).
⁶C. T. Sah and W. Shockley, Phys. Rev. 109, 1103 (1958).
⁷W. R. Wilcox, T. J. LaChapelle, and D. H. Forbes, J. Electrochem. Soc. 111, 1377 (1964).
⁸B. I. Boltaks, G. S. Kulikov, and R. Sh. Malkovitch, Fiz. Tverd. Tela 2, 181 (1960) [Sov. Phys. Solid State 2, 167 (1960)].
⁹Quoted in W. M. Bullis and F. J. Strieter, J. Appl. Phys. 39, 314 (1968).
¹⁰J. D. Struthers, J. Appl. Phys. 27, 1560 (1956).
¹¹C. B. Collins, R. O. Carlson, and C. J. Gallagher, Phys. Rev. 105, 1168 (1957).
¹²G. J. Sprokel and J. M. Fairfield, J. Electrochem. Soc. 112, 200 (1965).
¹³S. S. Li, Phys. Rev. 188, 1246 (1969).

Electron-Phonon Scattering in Te-Doped GaSb at Low Temperatures

P. C. Sharma and G. S. Verma

Department of Physics, Banaras Hindu University, Varanasi-5, India

(Received 24 February 1971)

The reduction in the thermal conductivity of Te-doped GaSb samples at temperatures below the maximum conductivity temperature is explained in detail by considering the scattering of phonons by conduction electrons. The Ziman model has been used to fit the phonon-conductivity results on Te-doped GaSb samples with excess donor-electron concentrations in the range $1.6\text{--}1.8 \times 10^{17} \text{ cm}^{-3}$, where the impurity levels merge with the conduction band. At low concentrations of the order $1.6 \times 10^{17} \text{ cm}^{-3}$ the phonons are scattered by electrons in the $\langle 000 \rangle$ minima band and at concentrations exceeding $1 \times 10^{18} \text{ cm}^{-3}$ the phonons are scattered by electrons in the $\langle 111 \rangle$ minima band. At intermediate concentrations phonons are scattered by electrons in both the bands.

I. INTRODUCTION

Recently, Poujade and Albany¹ studied the role of electron-phonon scattering in the phonon conductivity of Te-doped GaSb at low temperatures in the range $5\text{--}100^\circ \text{K}$. It was reported that at temperatures below the conductivity maximum at about 20°K , the addition of donor impurities drastically reduces the thermal conductivity. Further, the increase in the thermal resistivity was directly proportional to the donor-electron concentration. The change in the conductivity due to doping was attributed to electron-phonon scattering. Poujade and Albany¹ explored several possibilities in explaining the electron-phonon interaction, but did not give any quantitative explanation of their results below the conductivity maximum, where electron-phonon scattering makes a major contribution towards thermal resistance.

There are two types of electron-phonon interaction in doped semiconductors at low temperatures depending upon the state of electrons. One interaction is important for electrons which are in semi-isolated impurity states which are found when the carrier concentrations are less than 10^{17} cm^{-3} . The other is important when the electrons are in the well-defined impurity band which occurs at higher concentrations. In materials with sufficient-

ly high donor-electron concentration the impurity levels merge with the conduction band. The conduction electrons for such materials form a degenerate assemblage. Ziman² calculated the cross section for the scattering of phonons by electrons in a conduction band. The cross section depends upon the number of occupied donor electrons. He gave an expression for the relaxation rate of the electron-phonon scattering to satisfy the requirements that energy and momentum are conserved in the phonon-electron scattering. It is shown in the present work that quantitative explanation of the decrease in the values of phonon conductivity with doping, as well as its temperature dependence, can be obtained on the basis of Ziman's scattering for all the samples of Te-doped GaSb with donor-electron concentrations greater than 10^{17} cm^{-3} . One of the interesting conclusions of the present work is that at low donor-electron concentration of the order $1.6 \times 10^{17} \text{ cm}^{-3}$ the phonons are scattered by electrons in the $\langle 000 \rangle$ minima band. At concentrations exceeding $1 \times 10^{18} \text{ cm}^{-3}$, the phonons are scattered by electrons in the $\langle 111 \rangle$ minima band. At intermediate concentrations phonons are scattered by the electrons in both the bands, and one can predict, from the study of the density-of-states effective mass, the number of electrons in $\langle 000 \rangle$ and $\langle 111 \rangle$ minima bands.

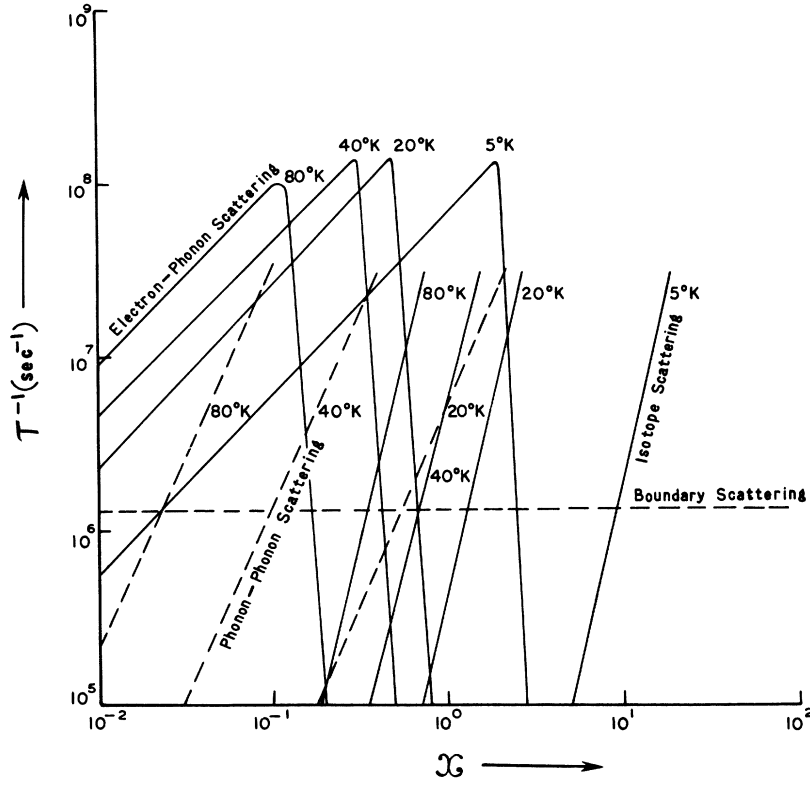


FIG. 1. Inverse of relaxation times for electron-phonon scattering, phonon-phonon scattering, boundary scattering, and scattering due to point defect are plotted against the dimensionless variable $x = \hbar\omega/k_B T$ for sample No. 34a.

II. ANALYSIS

Lattice thermal conductivity in the Callaway model³ at low temperatures is approximately

$$\kappa = C \int \frac{x^4 e^x / (e^x - 1)^2 dx}{\tau_c^{-1}},$$

where

$$C = \frac{k_B}{2\pi^2 v_s} \left(\frac{k_B T}{\hbar} \right)^3,$$

where v_s is the average phonon velocity and τ_c^{-1} is the inverse of combined relaxation time. Assuming the additivity of reciprocal relaxation times to hold good, one can write

$$\tau_c^{-1} = \tau_B^{-1} + \tau_{pt}^{-1} + \tau_{3ph,N}^{-1} + \tau_{3ph,U}^{-1} + \tau_{\theta p}^{-1},$$

where τ_{ep}^{-1} is the reciprocal of the relaxation time for electron-phonon scattering, $\tau_B^{-1} = L/v_s$ is the inverse of the relaxation time for boundary scattering of phonons, and L is a characteristic length of the crystal. $\tau_{3ph,N}^{-1}$ is the inverse of relaxation time for three-phonon normal processes and $\tau_{3ph,U}^{-1}$ is the inverse of relaxation time for three-phonon umklapp processes. These are given by

$$\begin{aligned} \tau_{3ph,N}^{-1} + \tau_{3ph,U}^{-1} &= (B_1 + B_2) \omega^2 T^3 \\ &= (B_1 + B_2) (k_B T / \hbar)^2 T^3 x^2, \end{aligned}$$

where τ_{pt}^{-1} is the reciprocal of relaxation time for point-defect scattering and is given by

$$\tau_{pt}^{-1} = \frac{V_0}{4\pi v_s^3} \left[\sum_i f_i \left(1 - \frac{m_i}{m} \right)^2 \right] \omega^4 = \frac{V_0 \Gamma}{4\pi v_s^3} \omega^4 = A\omega^4,$$

where V_0 is the atomic volume, m_i is the mass of the i th species of the atom, f_i is the fractional concentration of the i th species of the atom, and m is the average atomic mass.

Ziman's² relaxation time for the scattering of phonons by electrons is given by

$$\tau_{ep}^{-1} = DT \ln \frac{1 + \exp(\eta^* - N/T - PTx^2 + \frac{1}{2}x)}{1 + \exp(\eta^* - N/T - PTx^2 - \frac{1}{2}x)},$$

where

$$D = \epsilon^2 m^* k_B \delta^3 / 2\pi \hbar^4 M v_L, \quad N = m^* v_L^2 / 2k_B,$$

and

$$P = k_B / 8m^* v_L^2.$$

Here ϵ is the deformation potential constant, δ^3 is the atomic volume, M is the mean atomic weight, v_L is the longitudinal phonon velocity, and m^* is the electron effective mass.

In this treatment the phonon-creation processes which tend to balance out the annihilation processes to some extent were neglected. This effect is to increase the relaxation time by an amount which is

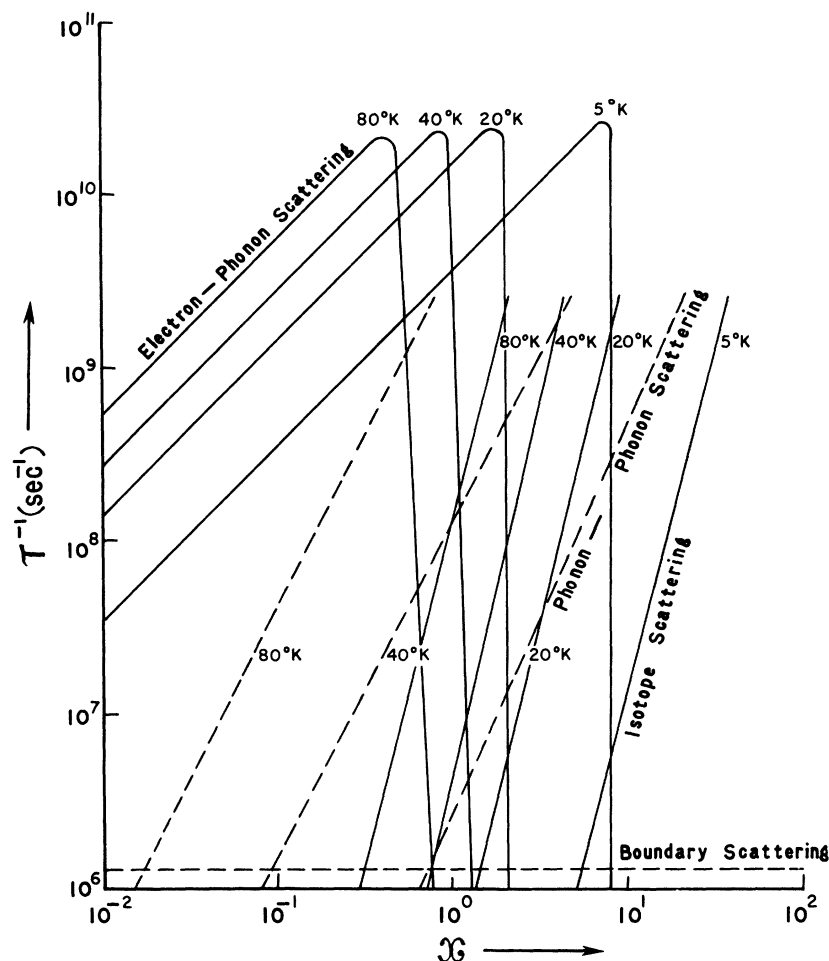


FIG. 2. Inverse of relaxation times for electron-phonon scattering, phonon-phonon scattering, boundary scattering, and scattering due to point defect are plotted against the dimensionless variable $x = \hbar\omega/k_B T$ for sample No. 40f.

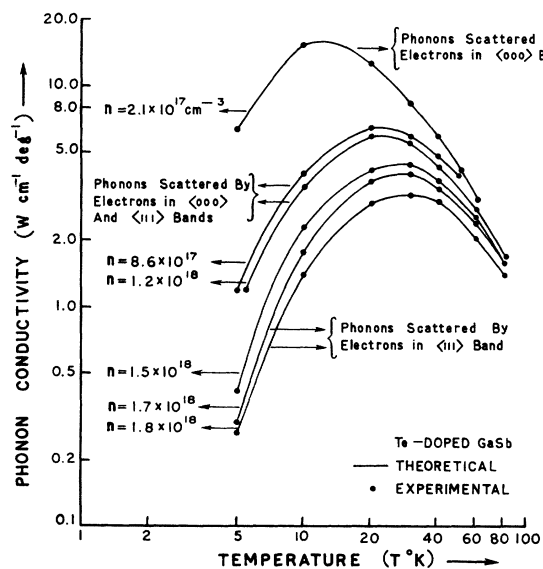


FIG. 3. Comparison of theoretical values of phonon conductivity with the experimental results in Te-doped GaSb sample Nos. $n 34a$, $n 58Cb_1$, $n 47f_2$, $n 76f$, $40d$, and $n 40f$ in the temperature range 2–80 °K.

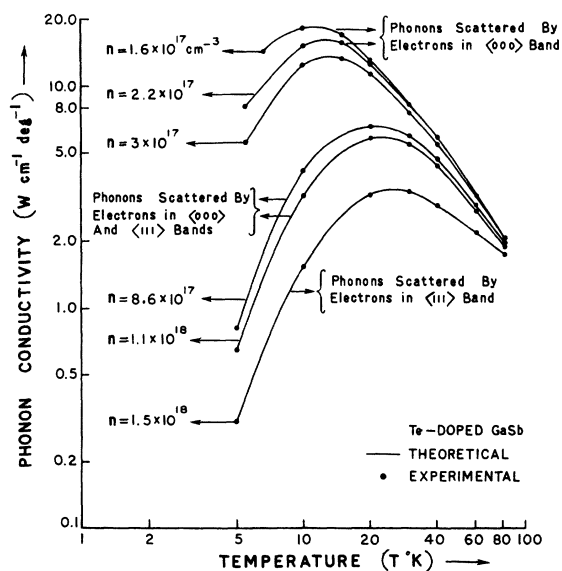


FIG. 4. Comparison of theoretical values of phonon conductivity with the experimental results in Te-doped GaSb sample Nos. $n 34d$, $n 34c$, $n 57e$, $n 74a$, $n 47c_2$, and $n 59Md$ in the temperature range 2–80 °K.

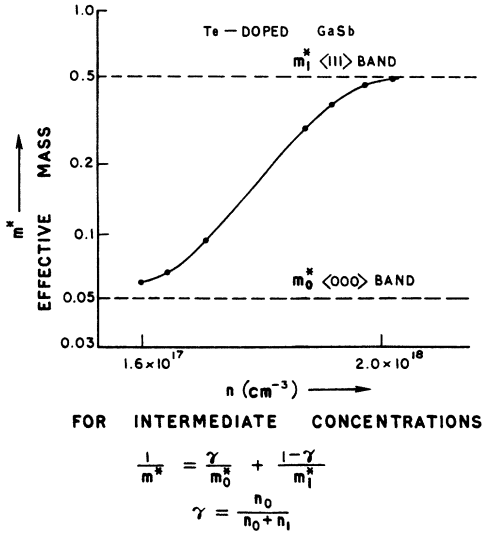


FIG. 5. Variation of density-of-states effective mass m^* with carrier concentration. At high donor electron concentrations ($2 \times 10^{18} \text{ cm}^{-3}$), m^* approaches m_1^* corresponding to electrons in the $\langle 111 \rangle$ minima band. At lower concentration ($1.6 \times 10^{17} \text{ cm}^{-3}$), m^* approaches m_0^* corresponding to electrons in the $\langle 000 \rangle$ band.

not significantly effective.

III. RESULTS AND DISCUSSIONS

The reciprocal of the relaxation times for electron-phonon interaction for the two typical samples are plotted in the Figs. 1 and 2 as a function of the dimensionless variable $x = \hbar\omega/k_B T$. It is observed that the cutoff in τ_{ep}^{-1} is sharpest at the lowest temperature. As the temperature increases the cutoff value of x decreases. The peak value of τ_{ep}^{-1} for every sample does not vary with the variation of temperature. For different values of the density-of-states effective mass, the peak values of τ_{ep}^{-1} will change. Our calculations show that as

TABLE I. Values of the various parameters used in the calculation of phonon conductivity of Te-doped GaSb samples.

$A = 0.813 \times 10^{-44} \text{ sec}^3$	$\Theta = 270 \text{ }^\circ\text{K}$
$(B_1 + B_2) = 0.7 \times 10^{-2} \text{ sec deg}^{-3}$	$v_L = 3.09 \times 10^5 \text{ cm/sec}$
$\epsilon = 16.3 \text{ eV}$	$E_f = 0.0517 \text{ eV}$
$\tau_B^{-1} = 1.226 \times 10^6 \text{ sec}^{-1}$	

the density-of-states effective mass decreases the peak value of τ_{ep}^{-1} decreases.

We find that a variation of the density-of-states effective mass explains the lattice-thermal-conductivity results of Te-doped GaSb samples very nicely without changing the other parameters. This may be seen from Figs. 3 and 4, where the theoretical values of phonon conductivity are compared with the experimental values. The values of the various parameters used in calculating the phonon conductivity are given in Tables I and II. Table II shows the values of the effective mass used to fit the data for different samples. The lowest value of m^* is 0.061 and the highest value of m^* is 0.488. Thus there is a variation in m^* of a factor of 7.

In GaSb, the lowest minimum in the conduction band occurs at $\vec{K} = 0$ and the subsidiary minima, which lie a little above this energy, occur in the $\langle 111 \rangle$ direction in \vec{K} space. The energy difference for the two minima is 0.084 eV. For the $K = 0$ minima, the density-of-states effective mass of the electrons is $m_0^* = 0.05$. Harland and Wooley⁴ have measured transverse magnetic resistance and Hall effect in Te-doped GaSb samples in the temperature range 4.2–300 °K and have interpreted their data in terms of the electrons in two sets of conduction minima at $\langle 000 \rangle$ and along $\langle 111 \rangle$ with effective masses $m_0^* = 0.0498$ –0.053 and $m_1^* = 0.50$, respectively.

If n_0 denotes the number of electrons in the

TABLE II. Values of density-of-states effective mass, electron concentration in $\langle 000 \rangle$ band, and electron concentration in $\langle 111 \rangle$ band for different samples of Te-doped GaSb having different carrier concentrations.

Sample	$n \text{ (cm}^{-3}\text{)}$	m^*	$n_0 \text{ (cm}^{-3}\text{)}$	$n_1 \text{ (cm}^{-3}\text{)}$
$n \ 40f$	1.8×10^{18}	0.488	0.00492×10^{18}	1.79508×10^{18}
$n \ 40d$	1.7×10^{18}	0.46	0.01642×10^{18}	1.58454×10^{18}
$n \ 59Md$	1.5×10^{18}	0.458	0.01528×10^{18}	1.48472×10^{18}
$n \ 76f$	1.5×10^{18}	0.41	0.03658×10^{18}	1.46342×10^{18}
$n \ 47f_2$	1.2×10^{18}	0.36	0.04633×10^{18}	1.15367×10^{18}
$n \ 47c_2$	1.1×10^{18}	0.36	0.04753×10^{18}	1.05247×10^{18}
$n \ 74a$	8.6×10^{17}	0.30	0.63704×10^{17}	7.96296×10^{17}
$n \ 58Gb_1$	8.6×10^{17}	0.30	0.63704×10^{17}	7.96296×10^{17}
$n \ 57e$	3.0×10^{17}	0.095	1.42095×10^{17}	1.57895×10^{17}
$n \ 34c$	2.2×10^{17}	0.067	1.57977×10^{17}	0.62023×10^{17}
$n \ 34a$	2.1×10^{17}	0.064	1.58958×10^{17}	0.51042×10^{17}
$n \ 34d$	1.6×10^{17}	0.061	1.27942×10^{17}	0.32058×10^{17}

$\langle 000 \rangle$ minima band and n_1 the number in the $\langle 111 \rangle$ band, then the total number of electrons is given by $n = n_0 + n_1$. Figure 5 shows the variation of m^* with n from Table II. It may be seen from this figure that m^* increases with the increase in n . One can also correlate the density-of-states effective mass m^* with m_0^* and m_1^* by the following relation:

$$1/m^* = \gamma/m_0^* + (1 - \gamma)/m_1^* ,$$

where

$$\gamma = n_0/(n_0 + n_1) = n_0/n .$$

Since the values of m_0^* and m_1^* are known from magnetoresistance measurements, it should be possible to calculate the number of electrons in the $\langle 111 \rangle$ minima band for a given value of n . Table II gives the values of n_0 and n_1 for different values of n . It may be seen from this table that at low concentrations of the order $1-2 \times 10^{17} \text{ cm}^{-3}$ the phonons are scattered by electrons in the $\langle 000 \rangle$ band. For large concentrations, n exceeding $1 \times 10^{18} \text{ cm}^{-3}$, the phonons are scattered by elec-

trons in the $\langle 111 \rangle$ minima band. For intermediate concentrations, the phonons are scattered by electrons from both the bands, and this is the reason that m^* lies in between the two extreme values 0.05 and 0.5. It may be further concluded that with the low electron concentrations the impurity states merge with the $\langle 000 \rangle$ minima band and with further increase in the concentration, they also merge with the $\langle 111 \rangle$ minima bands.

It is also concluded that the contribution of electron-phonon scattering to the lattice thermal resistance is maximum at the lowest temperature and a reduction is obtained at temperatures above the conductivity maximum.

It is also observed that electron-phonon scattering is strongly dependent on frequency and the low-frequency phonons are scattered most effectively.

ACKNOWLEDGMENTS

The authors express their thanks to Professor B. Dayal and Professor K. S. Singwi for their interest in this work. One of us (P. C. S.) is indebted to University Grants Commission India for the award of Research scholarship.

¹A. M. Poujade and H. J. Albany, Phys. Rev. **182**, 802 (1969).

²J. M. Ziman, Phil. Mag. **1**, 191 (1956).

³J. Callaway, Phys. Rev. **113**, 1046 (1959).

⁴Harland and Wooley, Can. J. Phys. **44-2**, 2715 (1966).

Nonequilibrium Steady-State Statistics and Associated Effects for Insulators and Semiconductors Containing an Arbitrary Distribution of Traps

J. G. Simmons and G. W. Taylor

Electrical Engineering Department, University of Toronto, Toronto, Canada

(Received 10 December 1970)

The statistics for an arbitrary distribution of traps under nonequilibrium steady-state conditions is derived, and it is seen to be identical in form to the Shockley-Read expression for a single trapping level. The energy dependence of the statistics has been investigated, and several interesting features have been deduced. It has been found appropriate to describe the occupancy of the traps in terms of two *modulated* Fermi-Dirac functions—one associated with trapped electrons, the other with trapped holes. It has been found possible to categorize the traps (into species) in terms of the ratio of their electron and hole capture cross sections. Detailed discussions are given for the electron and hole fillings of the traps as a function of energy, temperature, and illumination intensity for various trap distributions. The distinctions between shallow traps, recombination centers, and *dead* states are defined and discussed in detail.

I. INTRODUCTION

Shockley-Read¹ statistics have been extremely successful in describing nonequilibrium steady-state processes in semiconductors. The original work was concerned with the recombination pro-

cesses occurring through a single discrete trapping level. A formal extension of the theory, using the traditional Shockley-Read approach, to more than one distinct trapping level results in equations of extreme algebraic complexity.² As a result the problem has rarely been treated beyond this level